

Integrative Biology

Accepted Manuscript



This is an *Accepted Manuscript*, which has been through the Royal Society of Chemistry peer review process and has been accepted for publication.

Accepted Manuscripts are published online shortly after acceptance, before technical editing, formatting and proof reading. Using this free service, authors can make their results available to the community, in citable form, before we publish the edited article. We will replace this *Accepted Manuscript* with the edited and formatted *Advance Article* as soon as it is available.

You can find more information about *Accepted Manuscripts* in the [Information for Authors](#).

Please note that technical editing may introduce minor changes to the text and/or graphics, which may alter content. The journal's standard [Terms & Conditions](#) and the [Ethical guidelines](#) still apply. In no event shall the Royal Society of Chemistry be held responsible for any errors or omissions in this *Accepted Manuscript* or any consequences arising from the use of any information it contains.



Integrative Biology

ARTICLE

Apoptosis Progression Studied using Parallel Dielectrophoresis Electrophysiological Analysis and Flow Cytometry

H. J. Mulhall^a, A. Cardnell^a, K. F. Hoettges^{ab}, F. H. Labeed^a and M. P. Hughes^a

Received 00th January 20xx,
Accepted 00th January 20xx

DOI: 10.1039/x0xx00000x

www.rsc.org/

Apoptosis is characterised by many cellular events, but the standard Annexin-V assay identifies two; the transfer of the phospholipid phosphatidylserine (PS) from inner to outer leaflets of the plasma membrane, acting as an “eat me” signal to macrophages, and the permeabilisation of the membrane. In this paper we compare the results from the standard Annexin-V assay with electrophysiology data obtained in parallel using dielectrophoresis that highlights two changes in cell electrophysiology; a change in cytoplasmic conductivity which correlates with PS expression, whilst a membrane conductance spike that correlates with permeabilisation. Combining results from both methods shows a strong inverse relationship between conductivity and PS externalisation. One mechanism which may explain this correlation is related to intracellular Ca^{2+} , which is known to increase early in apoptosis. PS expression occurs when enzymes called scramblases swap external and internal phospholipids, and which are usually activated by Ca^{2+} , whilst the change in cytoplasmic conductivity may be due to K^+ efflux from intermediate conductance (IK) ion channels that are also activated by Ca^{2+} .

Introduction

Apoptosis, the process by which a cell self-destructs in a controlled fashion, is of fundamental importance to the maintenance of a healthy organism, with pathologies associated by either under- or over-occurrence of apoptosis. Of particular note in this is cancer, a disease often associated with cells losing the ability to self-destruct. Apoptosis itself is a highly complex process with many features, including changes in intracellular composition, the destruction of DNA, and the formation of apoptotic bodies. The process is orchestrated by multiple proteins, including caspases and cytochrome-c¹.

One of the early signs of apoptosis is the externalisation of the phospholipid phosphatidylserine (PS), which is usually found on the inner leaflet of the plasma membrane but which relocates to the outer leaflet during apoptosis². This negatively-charged phospholipid then acts as an “eat me” signal to macrophages to ensure cell removal. Translocation occurs through the action of membrane-bound enzymes called scramblases, which use calcium to activate the transfer of phospholipids between leaflets. However, there has been a belief that caspase-activated scramblases are required to play a role in apoptosis; an example of which was isolated recently³.

Another early process in apoptosis is a reduction in intracellular potassium ion concentration $[\text{K}^+]_i$, which precedes loss of membrane integrity⁴. $[\text{K}^+]_i$ decrease is associated with loss of water from the cell and apoptotic volume decrease (AVD). However, little is known

about the role of other monovalent ions during apoptosis and the relationship between changes in total intracellular ion concentration [total], and morphological and biochemical apoptotic events.

Arrebola et al.⁵ used quantitative electron probe X-ray microanalysis (EPXMA) to investigate simultaneous changes in Na, Cl and K ions during apoptosis. The group reported a decrease in $[\text{Cl}^-]_i$ and $[\text{K}^+]_i$ during apoptosis and a concomitant increase in $[\text{Na}^+]_i$. Although there is a body of work investigating changes in specific intracellular ion concentrations during apoptosis, there is currently little knowledge on total intracellular ion concentration [total], during apoptosis.

A new technique available to cell biological analysis is that of dielectrophoresis (DEP), a rapid, non-destructive and label-free technique by which it is possible to determine cell electrophysiology in many contexts⁶. It has already been exploited in the study of apoptosis⁷⁻⁹, particularly with regards to changes in the membrane^{10,11}. DEP offers many advantages over conventional methods of assessing cell electrophysiology such as patch-clamp; recent advances in DEP technology¹² have increased the speed and ease of use of the technique, allowing very rapid determination of the mean electrophysiological state of large numbers of cells simultaneously. This makes it much more suitable for the analysis of time-dependent effects such as drug action.

In this paper we analyse Jurkat cells induced into apoptosis using Staurosporine, comparing the expression on PS on the surface using Annexin-V with the cytoplasmic conductivity measured by DEP, both as a function of time and of drug concentration. The study shows that there is an inverse correlation between PS expression and intracellular conductivity that points to a common Ca^{2+} -mediated process driving both phenomena.

^a Centre for Biomedical Engineering, Department of Mechanical Engineering Sciences, University of Surrey, Guildford, Surrey GU2 7XH, United Kingdom.

^b Present address: Department of Electrical Engineering and Electronics, University of Liverpool, Liverpool, Merseyside L69 3BX, United Kingdom.

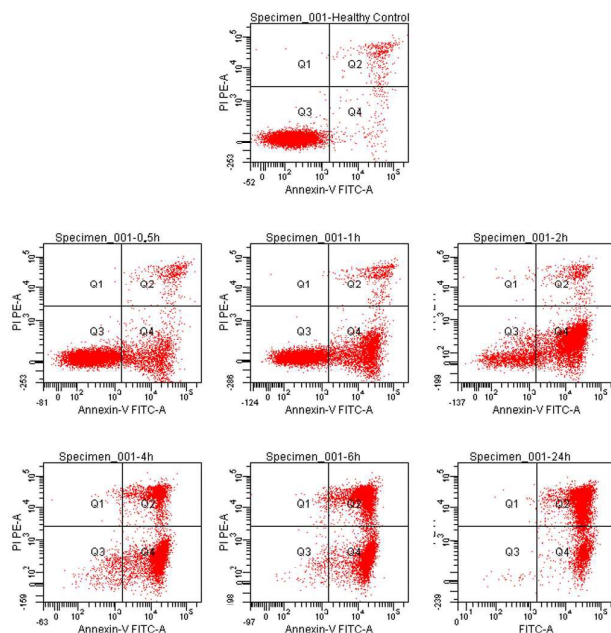


Figure 1. Jurkat cells were induced to undergo apoptosis after incubation with $0.5\mu\text{M}$ staurosporine for 0.5, 1, 2, 4, 6 and 24 hours. Increased expression of phosphatidylserine (PS) occurs in the early stage of apoptosis (quadrant 4) and increased propidium iodide dye uptake occurs in the late stage of apoptosis (quadrant 2).

Materials and Methods

Cell Culture

Jurkat cells were purchased from ATCC and cultured in RPMI 1640 supplemented with 10% foetal bovine serum (FBS), and subcultured every 48h. The cells were grown in a standard cell culture incubator at 5% CO_2 95% humidified air at 37°C . All cell culture products were purchased from Biosera (Ringmer, UK) unless otherwise stated.

Treatment with Apoptotic Inducing Agents

A stock solution of staurosporine (Sigma Aldrich, Poole, UK) was prepared by dissolving the agent in DMSO and aliquots were kept at -20°C . Jurkat cells were treated with $0.5\mu\text{M}$ staurosporine for 0.5, 1, 2, 4, 6 and 24 hours or with 0.01, 0.03, 0.05, 0.1, 0.3 and $0.5\mu\text{M}$ staurosporine for 2 hours at a concentration of 1×10^6 cells ml^{-1} . Solvent concentration in cell media was kept consistent at 0.5%.

Annexin V-FITC and PI Assays

An apoptosis detection kit consisting of both propidium iodide (PI) and fluorescein isothiocyanate (FITC)-conjugated annexin V was purchased from Sigma Aldrich (Poole, UK). Jurkat cells were treated with staurosporine and incubated for the desired time at 1×10^6 cells ml^{-1} . The cells were then washed twice with PBS and resuspended in 1x binding buffer at a concentration of 1×10^6 cells ml^{-1} . 500 μl of each cell suspension was then transferred to 12x75mm test tube (Fisher Scientific, Loughborough, UK). 5 μl of annexin V-FITC and 10 μl of PI were added to each cell suspension and incubated at room temperature, protected from light, for 10 minutes. The cells

were then held on ice until the fluorescence of cells was determined using a Becton Dickinson flow cytometer. All assays were repeated 5 times.

DEP Assay

DEP medium was prepared containing 248mM sucrose and 17mM D-glucose in deionised water^{13,14}. The conductivity of the medium was adjusted to 0.01S m^{-1} by addition of PBS (Biosera, UK) and verified by a Jenway 470 conductivity meter (VWR Jencons, UK). Jurkat cells were harvested from culture vessels and centrifuged at 200g for 5 minutes. The cells were then washed twice by centrifugation in DEP experimental medium and resuspended at a concentration of 5×10^6 cells ml^{-1} . Cell viability was measured using trypan blue assay. Cell radii were obtained by capturing images of at least 50 cells per experiment on a haemocytometer and measuring the cell diameter using image analysis software.

A prototype 3DEP (DEPtech, Uckfield UK) DEP-microwell electrode system was used to determine the electrophysiological properties of Jurkat cells. The fabrication of the DEP-microwell and experimental methods are described in detail elsewhere^{12,15,16}. Briefly, for each experiment, cell motion was measured in response to a non-uniform AC electric field for five frequencies per decade from 1kHz to 20MHz. A MatLab (The Mathworks Inc, Nantick USA) script was used to assess cell distribution in the DEP-microwell over the duration of time that the electric potential was applied. The electrophysiological properties were derived by fitting a 'single-shell' model to the line of best fit through the electrophysiological spectra^{17,18}. The line of best fit had a correlation co-efficient of 0.95 or above for all experiments. All DEP experiments were repeated 5 times.

Results

Studies of apoptosis were performed for multiple concentrations at a fixed time (2h), and for multiple times at a fixed concentration of STS ($0.5\mu\text{M}$). Considering the former case, Jurkat cells were induced to undergo apoptosis after incubation with $0.5\mu\text{M}$ staurosporine for 0.5, 1, 2, 4, 6 and 24 hours (Figure 1). Increased expression of phosphatidylserine (PS), associated with the early stage of apoptosis (quadrant 4) was observed within 0.5h of incubation; subsequent, simultaneous increased propidium iodide dye uptake (quadrant 2) correlated to the late stage of apoptosis was observed in all samples (even the healthy control) in small numbers, but became considerably more prominent after 4h of exposure. When the populations of each quadrant were plotted (Figure 2a), it could be seen that early apoptotic cells were most numerous after 2h, whereas the populations in early and late apoptosis remained largely constant from 6-24h. All cells had entered apoptosis by 4h.

Similar analysis for drug concentrations between 0.01- $0.5\mu\text{M}$ and fixed incubation for two hours (Figure 2b) showed that a proportion of Jurkat cells entered early apoptosis at all drug concentrations, ranging between approximately 10%-80% of cells across the concentration range. However, late stage apoptosis, characterised by uptake of propidium iodide, did not occur above a basal level for any of the STS concentrations and incubation period used in this study. Therefore, at these concentrations and incubation times, changes in electrophysiological properties were associated with early, not late stage apoptotic events.

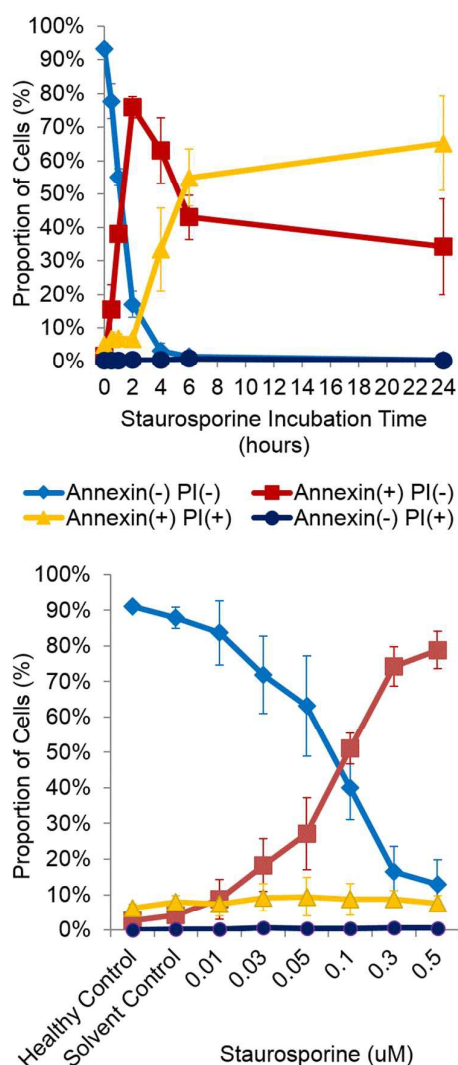


Figure 2. Proportions of cells identified at different phases of apoptosis. Incubation with staurosporine (STS) (a) at a concentration of 0.5 μM for 0.5, 1, 2, 4, 6 and 24 hours and (b) at concentrations between 0.01-0.5 μM for two hours, induced Jurkat cells to undergo apoptosis. The proportion of Jurkat cells in early apoptotic stage, characterised by externalisation of phosphatidylserine, increases with increasing concentrations of STS whereas the proportion of healthy cells decreases. Late stage apoptosis, characterised by uptake of propidium iodide, did not occur above a basal level for the STS concentrations and incubation period used in this study. The proportion of Jurkat cells in late apoptotic/necrotic and necrotic stage remained relatively constant over all concentrations. Error bars indicate standard deviations.

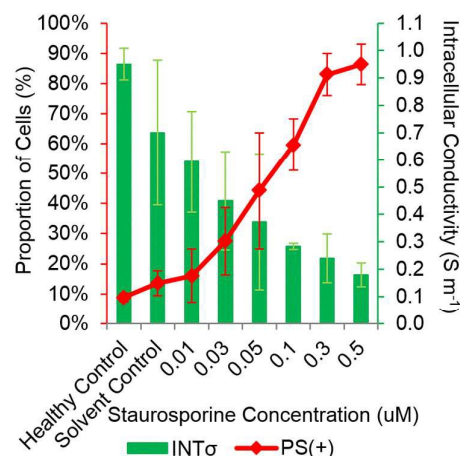


Figure 3. The proportion of Jurkat cells exhibiting PS externalisation after 2h incubation with staurosporine, plotted with the cytoplasmic conductivity in the same cell populations as determined by DEP. Error bars indicate standard deviations.

In parallel with flow cytometric analysis, DEP was used to determine the electrophysiological properties of the cells. Considering first the cells incubated with 0-0.5 μM STS for 2h (Figure 3) showed a variation in electrophysiology with drug concentration, with an inverse correlation being observed between the proportion of cells in early phase apoptosis, as characterised by phosphatidylserine externalisation, and the conductivity of the cell interior (σ_{INT}). This parameter relates to the number of free ions in the cytoplasm and loosely correlates with membrane potential¹⁹. Commonly, a loss of ionic content is associated with membrane permeabilisation, allowing the cytoplasm contents to escape; whilst it is possible that σ_{INT} measurements could be influenced by a loss in membrane integrity, viable cell membranes are not permeable to PI, allowing PI uptake to provide a marker for membrane function. PI fluorescence was not observed to increase above baseline (Figure 2b), indicating the presence of intact cell membranes and suggesting that the changes in σ_{INT} could not be attributed to loss of membrane integrity.

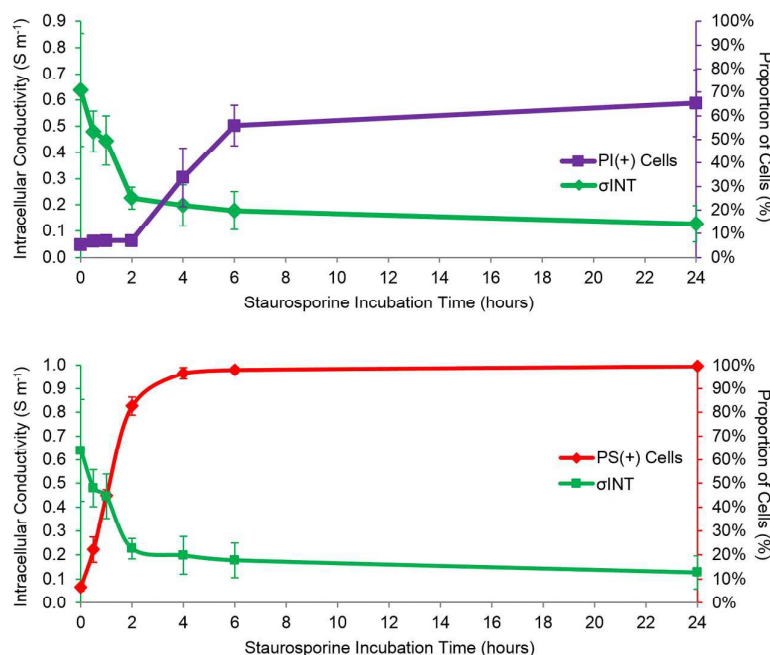


Figure 4. When Jurkat cells are incubated with staurosporine (STS), intracellular conductivity decreases as the proportion of cells in early apoptosis, characterised by phosphatidylserine (PS) externalisation, increases. Propidium iodide expression (indicating membrane permeabilisation) lags behind the conductivity decrease, indicating that permeabilisation is not the source of the conductivity change. Error bars indicate standard deviations.

In order to investigate this further, the change in cytoplasmic conductivity and effective membrane capacitance and conductance were investigated at a fixed concentration of 0.5 μ M STS at multiple time points over a 24h period and compared with both PS and PI expression, as can be seen in figures 4 and 5. Cell radii of 100 cells at each time point were also measured (figure 5) Considering first the cytoplasm conductivity and comparing the Annexin/PI and DEP data (figure 4), it can be seen that the reduction in cytoplasm conductivity is coincident with the increase in rise in PS expression, but *precedes* the increase in uptake of PI by late-apoptotic cells by 4h – again reinforcing the indication that the change in ionic strength is not related to ion leakage through membrane permeabilisation, but instead reflects an ordered cellular processes. The cell radii showed a reduction from 5.7 μ m to 4.5 μ m during the first four hours, after which they remained stable. This is commensurate with other observations, where cells in early apoptosis shrink as water is lost to maintain osmotic balance after significant ion loss⁷. Membrane capacitance per unit remained relatively stable throughout, beginning at 9.1 mFm⁻² and varying within $\pm 12\%$ of this value throughout the experiment, ending at 8.0 mFm⁻²; slight elevation simultaneous to radius decrease indicates increased membrane folding due to “wrinkling” as the cell shrinks. Finally, whilst the membrane conductance per unit area remained within 10% of the initial value (1179 Sm⁻²) for much of the experiment, a large spike corresponding to a peak 40% uplift in membrane conductance was observed between 2-4h after treatment. The timing suggests that this elevation may be coincident with the increase in PI expression and hence more likely to be due to ion permeability due to the presence of membrane pores than due to ion channel activity.

Discussion

Expression of PS on the outer leaflet of the plasma membrane is associated with scramblase activity; scramblases are membrane-bound enzymes which transport phospholipids between inner and outer leaflets of the membrane and are commonly driven by calcium in the cytoplasm^{20,21}, though a class of caspase-activated scramblases were reported recently³. As scramblase activity does not affect intracellular ion concentration beyond the calcium binding required to activate the enzyme, it can be assumed that the relation between PS expression and cytoplasmic conductivity exhibits correlation without causation; however, there may be an underlying mechanism that activates both.

It is known⁴ that a reduction in intracellular potassium [K⁺]_i and sodium [Na⁺]_i ion concentration occurs during apoptosis and precedes loss of membrane integrity (necrosis), which has been implicated in changes in cytoplasmic conductivity during apoptosis in the past⁷. Potassium is the most common free-charge carrier in the cytoplasm, but reduces in concentration from ~ 140 mM to 30-50 mM during apoptosis²²; notably, this proportional decrease in ion content mirrors the change in cytoplasmic conductivity seen in figure 4, from ~ 0.7 mSm⁻¹ to 0.2 mSm⁻¹; however, other ionic traffic such as Na⁺ efflux or even Ca²⁺ or Cl⁻ influx, make direct assignation of the conductivity change to one ion species impossible.

It is understood that Ca²⁺ trafficking plays a significant role in apoptosis, governing the release of cytochrome c for example²³. Recent work by McFerrin et al.²⁴ has indicated that apoptotic potassium efflux occurs through Ca²⁺-activated intermediate-conductance potassium (IK) channels. Apoptosis is a deeply complex sequence of events, such that there is the possibility that calcium-driven K⁺ efflux might simply be coincident with

independent, caspase-driven scramblase activity. However, given the far more prolific nature of calcium-driven scramblases, it could be suggested that both activities occur as a direct result of intracellular calcium increase as part of the apoptotic cascade. However, other explanations may exist – for example, Ca^{2+} is also thought to contribute to cause a reduction in ATP production in mitochondria, which could lead to a reduction in cytoplasm ions and hence a reduction in cytoplasm conductivity.

One notable aspect of the result is the difference between the observation that the cytoplasmic conductivity reduces in apoptosis in STS-treated Jurkat cells, but increased in K562 cells treated with the same agent^{7,8}. However, one significant difference in the responses is that the K562 cells reduced in size very rapidly after treatment, to which the rise in conductivity following K^{+} efflux was attributed; it was suggested that concomitant water efflux caused concentration of the remaining intracellular charge, raising the conductivity⁸. In the Jurkat experiments, however, the corresponding change in cell size was small and relatively short-

lived, indicating that this concentration effect was not seen. Furthermore, this result also follows observations in HL-60 cells undergoing apoptosis, where cytoplasmic conductivity was also seen to reduce¹⁰.

We had also anticipated the visible presence of multiple subpopulations in the DEP spectra of apoptotic cells, as had been observed in our previous work on the subject⁷. However, when modelled, the data showed greatest correlation when modelled as a single population. Whilst DEP can detect multiple populations it is not as accurate as flow cytometry in doing so; whilst it is possible to detect different cells in a population when they constitute as little as 10% of the population¹², this tends to be where the differences are substantial (such as between live and dead cells); as such, 10% represents about the detectable threshold for subpopulation detection. If we consider the proportions of cells at different apoptotic states at 2h (figure 2a) then ca. 80% of cells are in early apoptosis, 10% healthy and 10% late apoptosis. This would mean the contribution of the cells outside early apoptosis would be sufficiently low in number to be excluded from the analysis, leaving the early apoptotic population to dominate. An additional point to consider is that the extent of PS externalisation is a continuum rather than binary state; once scramblase activity starts, PS begins appearing on the cell surface in greater quantities as time passes. Considering Figure 1, cells begin in Q1 but then drift to Q2. This shift may result in a spectrum corresponding to mean of the population, rather than the appearance of two separate populations; since the position in the continuum relates to the degree of PS expression detected by the Annexin assay, this would still relate *mean* cytoplasmic conductivity with PS externalisation.

Conclusions

In the quest for a complete understanding of the nature of the apoptotic process, there are still significant gaps in understanding the mechanisms underpinning the activation of the PS-driven “eat me” response, particularly with regard to the nature of scramblase activation. Here, we indicate that there is a strong correlation between scramblase activity and Ca^{2+} -driven IK^{+} pumps during apoptosis, indicating that calcium, rather than caspase, may be the primary driver of scramblase during apoptosis.

Acknowledgements

This work was funded by Labtech International and Finance South East. The authors thank Dr Lisi Meira for valuable discussions.

References

- 1 Elmore S, Apoptosis, a review of programmed cell death. *Toxicol. Pathol.* 2007, 35, 495-516.
- 2 Martin SJ, Reutelingsperger CEM, McGahon AJ, Rader JA, Schiew RCAAV, Laface DM and Green DT, Early Redistribution of Plasma Membrane Phosphatidylserine Is a General Feature of Apoptosis Regardless of the Initiating Stimulus, Inhibition by Overexpression of Bcl-2 and Abl. *J. Exp. Med.* 1995, 182, 1545-1556.
- 3 Suzuki J, Denning DP, Imanishi E, Horvitz R and Nagata S, Xk-Related Protein 8 and CED-8 Promote Phosphatidylserine Exposure in Apoptotic Cells *Science* 2013, 341, 403-406.
- 4 Bortner CD, Hughes FM and Cidlowski JAA, Primary Role for K^{+} and Na^{+} Efflux in the Activation of Apoptosis. *J Biol. Chem.* 1997, 272, 32436-32442. C. D. Bortner and J. A.

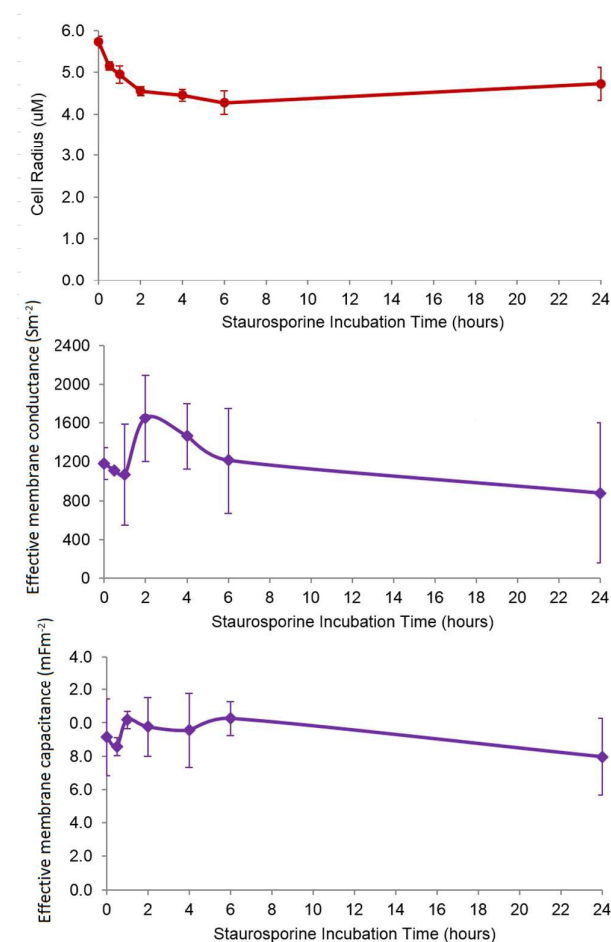


Figure 5. Variations in mean values of cell radius, and effective membrane conductance and capacitance per unit area, as a function of time after staurosporine exposure. Error bars indicate standard deviations.

- Cidlowski, "Ion channels and apoptosis in cancer," *Philosophical Transactions of the Royal Society B: Biological Sciences*, vol. 369, no. 1638, pp. 20130104–20130104, Feb. 2014.
- 5 Arrebola F, Zabiti S, Cañizares FJ, Cubero MA, Crespo PV and Fernández-Segura E, Changes in Intracellular Sodium, Chlorine, and Potassium Concentrations in Staurosporine-Induced Apoptosis. *J. Cell. Physiol.* 2005, 204, 500-507.
 - 6 Pethig R, Dielectrophoresis, status of the theory, technology, and applications. *BiOMICROfluidics*. 2010, 4, 022811.
 - 7 Labeed FH, Coley HM and Hughes MP, Differences in the biophysical properties of membrane and cytoplasm of apoptotic cells revealed using dielectrophoresis *Biochim. Biophys. Acta* 2006, 1760, 922-929.
 - 8 Chin S, Hughes MP, Coley HM and Labeed FH, Rapid assessment of early biophysical changes in K562 cells during apoptosis determined using dielectrophoresis *Int. J. Nanomed.* 2006, 1, 333-337
 - 9 Lv Y, Zeng LQ, Zhang GB, Xu YC, Lu Y, Mitchelson K, et al., Systematic dielectrophoretic analysis of the Ara-C-induced NB4 cell apoptosis combined with gene expression profiling *Int. J. Nanomed.* 2013, 8, 2333-2350.
 - 10 Wang XJ, Becker FF and Gascoyne PRC, Membrane dielectric changes indicate induced apoptosis in HL-60 cells more sensitively than surface phosphatidylserine expression or DNA fragmentation *Biochim Biophys. Acta* 2002, 1564, 412-420.
 - 11 Pethig R and Talarzy MS, Dielectrophoretic detection of membrane morphology changes in Jurkat T-cells undergoing etoposide-induced apoptosis. *IET Proc Nanobiotechnol.* 2007, 1, 2-9
 - 12 Hoettges KF, Hubner Y, Broche LM, Ogin SL, Kass GEN and Hughes MP, Dielectrophoresis-Activated Multiwell Plate for Label-Free High-Throughput Drug Assessment. *Anal. Chem.* 2008, 80, 2063-2068; Broche PM, Hoettges KF, Ogin SL, Kass GEN and Hughes MP. Rapid, automated measurement of dielectrophoretic forces using DEP-activated microwells. *Electrophoresis* 2011, 32, 2393-2399
 - 13 Gascoyne PRC, Pethig, R, Burt JPH and Becker, FF, Membrane Changes Accompanying the Induced Differentiation of Friend Murine Erythroleukemia Cells Studied by Dielectrophoresis. *Biochim. Biophys. Acta* 1993, 1149, 119-126.
 - 14 Pethig R, Jakubek LM, Sanger RH, Heart E, Corson ED and Smith PJS, Electrokinetic Measurements of Membrane Capacitance and Conductance for Pancreatic Beta-Cells. *IEE Proc. Nanobiotechnol.* 2005, 152, 189-193.
 - 15 Broche LM, Labeed FH and Hughes MP, Extraction of Dielectric Properties of Multiple Populations from Dielectrophoretic Collection Spectrum Data. *Phys. Med. Biol.* 2005, 50, 2267-2274.
 - 16 Hubner Y, Hoettges KF, Kass GEN, Ogin SL and Hughes MP, Parallel Measurements of Drug Actions on Erythrocytes by Dielectrophoresis, Using a Three-Dimensional Electrode Design. *IEE Proc. Nanobiotechnol.* 2005, 152(4), 150-154.
 - 17 Irimajiri A, Hanai T and Inouye A, Dielectric Theory of Multi-Stratified Shell-Model with Its Application to a Lymphoma Cell. *J. Theor. Biol.* 1979, 78, 251-269.
 - 18 Huang Y, Wang X-B, Becker FF and Gascoyne PRC, Membrane Changes Associated with the Temperature-Sensitive P85gag-Mos-Dependent Transformation of Rat Kidney Cells as Determined by Dielectrophoresis and Electrorotation. *Biochim. Biophys. Acta* 1996, 1282, 76-84
 - 19 Coley HM, Labeed FH, Thomas H and Hughes MP, Biophysical characterization of MDR breast cancer cell lines reveals the cytoplasm is critical in determining drug sensitivity *Biochim. Biophys. Acta* 2007, 1770, 601-608.
 - 20 Leventis PA and Grinstein S, The Distribution and Function of Phosphatidylserine in Cellular Membranes *Ann. Rev. Biophys.* 2010, 39, 407-427.
 - 21 Suzuki J, Umeda M, Sims PJ and Nagata M, Calcium-dependent phospholipid scrambling by TMEM16F *Nature* 2010, 468, 834–838.
 - 22 Park I-S and Ja –Eun K, Potassium Efflux During Apoptosis *J. Biochem. Mol. Biol.* 2002, 35, 41-46. F. M. Hughes Jr and J. A. Cidlowski, "Potassium is a critical regulator of apoptotic enzymes in vitro and in vivo," *Advances in enzyme regulation*, vol. 39, no. 1, pp. 157–171, 1999.
 - 23 Mattson MP and Chan SL, Calcium Orchestrates Apoptosis *Nat Cell Biol.* 2003, 5, 1041-1043. K. Dezaki, E. Maeno, K. Sato, T. Akita, and Y. Okada, "Early-phase occurrence of K⁺ and Cl[–] efflux in addition to Ca²⁺ mobilization is a prerequisite to apoptosis in HeLa cells," *Apoptosis*, vol. 17, no. 8, pp. 821–831, Aug. 2012. C. S. I. Nobel, J. K. Aronson, D. J. van den Dobbelsteen, and A. F. Slater, "Inhibition of Na⁺/K⁺-ATPase may be one mechanism contributing to potassium efflux and cell shrinkage in CD95-induced apoptosis," *Apoptosis*, vol. 5, no. 2, pp. 153–163, 2000.
 - 24 McFerrin MB, Turner KL, Cuddapah VA and Sontheimer H, Differential role of IK and BK potassium channels as mediators of intrinsic and extrinsic apoptotic cell death. *Am J Physiol Cell Physiol* 2012, 303, C1070-1078. S. P. Yu, L. M. Canzoniero, and D. W. Choi, "Ion homeostasis and apoptosis," *Current opinion in cell biology*, vol. 13, no. 4, pp. 405–411, 2001. S. P. Yu, "Regulation and critical role of potassium homeostasis in apoptosis," *Progress in Neurobiology*, vol. 70, no. 4, pp. 363–386, Jul. 2003.